



# Depiction of an external classical field effects on a four-level W-configuration atom embedded in a coherent cavity field

S. I. Ali<sup>1</sup>

Received: 12 March 2023 / Accepted: 15 May 2023 / Published online: 14 June 2023  
© The Author(s) 2023

## Abstract

This paper examines the dynamics of a W-configuration four-level atom in a quantized cavity field and the system driven by an external classical field. By applying some canonical transformations, we derive analytical solutions to the Schrödinger equation for the corresponding Hamiltonian. We have analyzed the impact of the external field and detuning parameters on the system's relative entropy of coherence, Wigner function, and Pancharatnam phase. Our findings suggest that the external field parameter greatly affects the coherence of the system, whereas the detuning parameters may increase its maximum bounds. Furthermore, we have utilized the Wigner function as a tool to measure the quantumness and classicality of the system in its phase space. Our results indicate that the external field has a greater impact on the classicality of the system than the detuning parameters. Additionally, we have observed rapid oscillations in the dynamics of the Pancharatnam phase for large detuning values. It is worth noting that the external field reduces the number of phase jumps in the system.

**Keywords** Four-level atom · Wigner function · Pancharatnam phase · External classical field · Coherence

## 1 Introduction

Quantum systems of atom–field interaction are an increasingly significant area of research in quantum physics. The intricate relationship between atoms and electromagnetic fields has been studied in great detail, and this research has yielded significant progress in both theory and practical application. In particular, insights gained from this research have revolutionized our understanding of how light interacts with matter on an atomic level, and enabled us to comprehend the behavior of complex molecules [1]. Rabi model is a semi-classical model that has been widely studied and has yielded a deep understanding of the behavior of atoms and their interactions with electromagnetic fields [2]. This model has been used to provide explanations for phenomena, such as Rabi oscillations and the Lamb shift [3]. Due to its broad applicability, the Rabi model continues to be a key tool for researchers in the field of quantum optics. The second most important model was proposed in 1963 by physicists E.T. Jaynes and F.W. Cummings to describe the

interaction between a single atom and a single photon [4]. Since its conception, it has been prominently used to explore a variety of physical phenomena, including superconductivity and quantum computation [5]. The Jaynes–Cummings model has been greatly expanded over the years, allowing for more intricate interactions between atoms and fields, as well as multiple modes of the field [6], through the addition of multiple atoms, external terms and non-linear interactions [7–11]. In essence, the generalization of the Jaynes–Cummings model has enabled scientists to explore a variety of possibilities that were previously not available. In particular, the interaction between a fourth-level atom and a quantized field, which is one of these generalizations, can be used to study phenomena, such as lasing, photon blockade and entanglement [12]. Additionally, this type of interaction has been used to explore the behavior of quantum systems in the presence of an external driving field and a Kerr-like non-linear medium [13].

Quantum coherence is an important concept in quantum mechanics and information processing, which describes the ability of a quantum system to remain in a superposition of multiple states [14]. It is the basis for many phenomena, such as entanglement and interference [15]. Coherence is a measure of how well the system maintains its quantum state over time. In other words, it is a measure of how well the

✉ S. I. Ali  
salama5laser@azhar.edu.eg

<sup>1</sup> Mathematics Department, Faculty of Science, Al-Azhar University, Nasr City 11884, Cairo, Egypt

system can maintain its quantum properties without being disturbed by external influences. Coherence has been studied extensively in recent years and has been found to be essential for many quantum systems, such as nonlinear  $SU(1, 1)$  quantum states [16], two-qubit system interacting with a deformed cavity [17], two coupled quantum dot molecules [18], and accelerated systems [19, 20].

The quantum Wigner function (W-function) is a mathematical tool originally proposed by Eugene Wigner in 1932, used to describe the quantum states of particles, such as atoms and photons [21]. This function has been used to gain insights into the quantum interference of particles, quantum system dynamics, and the interaction between atoms and light fields [22]. It has been applied across many different areas of quantum physics and has been used in recent research to control atomic and field states, such as, the classicality/ non-classicality of three qubit system [23, 24], negativity of multimode non-Gaussian states [25], and quantum correlation of light-matter interaction [26, 27]. Furthermore, the W-function has proven to be invaluable for studying the effects of atom-field interactions on atomic states, which is critical for the development of quantum technologies [28].

Building on previous studies, this paper aims to explore how an external classical field affects a W four-level atom placed in a quantized cavity field. In order to solve the physical Hamiltonian, we require certain approximations and rotations when subjecting the system to an external classical field. In our paper, we have employed a method that entails fewer approximations compared to existing approaches for solving the system. This is due to the difficulty in obtaining an exact solution for a quantum system with high dimensionality in the presence of a classical field [29]. Notwithstanding the existing research, this system continues to draw interest from both experimental and theoretical scientists, particularly with respect to its statistical properties and quantum correlations. Furthermore, the model and results presented in this study are both intriguing and promising for future research. For instance, it can be utilized to investigate the four wave mixing process, both theoretically and experimentally [30]. Notably, the observation of the tripod-configuration for a four-level atom has been instrumental in enhancing the cross-phase modulation based on a double electromagnetically induced transparency [31]. Therefore, we present a physical model and demonstrate an exact solution system in Sect. 2. In Sect. 3, 4 and 5, we discuss the mathematical quantum quantifiers associated with our model, where we defined the relative entropy of coherence, Wigner function, and Pancharatnam phase. Finally, our results are summarized and discussed in Sect. 6.

## 2 Hamiltonian system

Assuming the physical system consists of interaction of a single W configuration of a four-level atom inside a single mode of a quantized field and an external classical laser field. Considering the transitions between the atomic levels are  $|1\rangle \leftrightarrow \{|3\rangle, |4\rangle\}$ , and  $|2\rangle \leftrightarrow \{|3\rangle, |4\rangle\}$ , where  $|1\rangle, |4\rangle$  are the upper and ground states respectively, while  $|2\rangle, |3\rangle$  are the two intermediate states. The classical field associates the upper and lower state with two intermediate states. Under the rotating wave approximation, the physical model that describes Hamiltonian system is written as ( $\hbar = 1$ ),

$$\hat{H} = \hat{H}_0 + \hat{H}_I + \hat{H}_D, \tag{1}$$

where

$$\begin{aligned} \hat{H}_0 &= \omega_f \hat{a}^\dagger \hat{a} + \sum_{i=1}^4 \omega_i \hat{\sigma}_{ii}, \\ \hat{H}_I &= \lambda_1 (\hat{a} (\hat{\sigma}_{13} + \hat{\sigma}_{14} + \hat{\sigma}_{23} + \hat{\sigma}_{24}) + \text{h.c.}), \\ \hat{H}_D &= \lambda_2 (\hat{\sigma}_{12} + \hat{\sigma}_{34} + \text{h.c.}). \end{aligned}$$

Here,  $\omega_f$  and  $\omega_i$  are the frequencies of the cavity field and atomic levels transition, respectively.  $\hat{a}$  and  $\hat{a}^\dagger$  are the bosonic annihilation and creation of the cavity field.  $\hat{\sigma}_{ji} = |j\rangle\langle i|$  are polarization operators for  $i \neq j$  and free atomic operators for  $i = j$ .  $\lambda_1$  and  $\lambda_2$  represent the coupling constants of the atom-field and external field, respectively. The classical field is represented by the transition from  $|1\rangle$  to  $|2\rangle$  and from  $|3\rangle$  to  $|4\rangle$ . Via denationalization for the free atomic subsystem  $\sum_{i=1}^4 \omega_i \hat{\sigma}_{ii}$  and the driven Hamiltonian  $\hat{H}_{\text{driven}}$ , one can obtain the following eigenstates,

$$\begin{bmatrix} |1\rangle \\ |2\rangle \\ |3\rangle \\ |4\rangle \end{bmatrix} = \begin{bmatrix} \beta_1^- & \beta_1^+ & 0 & 0 \\ \beta_2^- & \beta_2^+ & 0 & 0 \\ 0 & 0 & \alpha_1^- & \alpha_1^+ \\ 0 & 0 & \alpha_2^- & \alpha_2^+ \end{bmatrix} \begin{bmatrix} |l_1\rangle \\ |l_2\rangle \\ |l_3\rangle \\ |l_4\rangle \end{bmatrix}, \tag{2}$$

where

$$\begin{aligned} \beta_1^\pm &= \frac{\Delta_1 \pm \sqrt{\Delta_1^2 + 4\lambda_2^2}}{\sqrt{4\lambda_2^2 + (\Delta_1 \pm \sqrt{\Delta_1^2 + 4\lambda_2^2})}}, & \beta_2^\pm &= \frac{2\lambda_2}{\sqrt{4\lambda_2^2 + (\Delta_1 \pm \sqrt{\Delta_1^2 + 4\lambda_2^2})}}, \\ \alpha_1^\pm &= \frac{\Delta_2 \pm \sqrt{\Delta_2^2 + 4\lambda_2^2}}{\sqrt{4\lambda_2^2 + (\Delta_2 \pm \sqrt{\Delta_2^2 + 4\lambda_2^2})}}, & \alpha_2^\pm &= \frac{2\lambda_2}{\sqrt{4\lambda_2^2 + (\Delta_2 \pm \sqrt{\Delta_2^2 + 4\lambda_2^2})}}, \\ \text{and} \quad \Delta_1 &= \omega_1 - \omega_1, & \Delta_2 &= \omega_3 - \omega_4. \end{aligned}$$

However, the atomic levels  $|1\rangle, |2\rangle, |3\rangle, |4\rangle$  of the atomic flip operators  $\hat{\sigma}_{ij}$  in eq. (2) can be transformed into a new rotating levels  $|l_1\rangle, |l_2\rangle, |l_3\rangle, |l_4\rangle$ . Hence, the the atomic flip operators  $\hat{\sigma}_{ij}$  may be transformed into  $\hat{S}_{ij} = |l_i\rangle\langle l_j|$ , which obey the commutation relation  $[\hat{S}_{ij}, \hat{S}_{nm}] = \hat{S}_{im} \delta_{nj} - \hat{S}_{nj} \delta_{im}$ .

Moreover, Hamiltonian (1) in the new rotating bases may be written as,

$$\hat{H} = \omega_f \hat{a}^\dagger \hat{a} + \Omega_1 \hat{S}_{11} + \Omega_2 \hat{S}_{22} + \Omega_3 \hat{S}_{33} + \Omega_4 \hat{S}_{44} + \hat{a}(\mu_1 \hat{S}_{13} + \mu_2 \hat{S}_{14} + \mu_3 \hat{S}_{23} + \mu_4 \hat{S}_{24}) + h.c., \tag{3}$$

with the new atomic transitions,

$$\begin{aligned} \Omega_1 &= \omega_1 \beta_1^{-2} + \omega_2 \beta_2^{-2} + 2\lambda_2 \beta_1^- \beta_2^-, \\ \Omega_2 &= \omega_1 \beta_1^{+2} + \omega_2 \beta_2^{+2} + 2\lambda_2 \beta_1^+ \beta_2^+, \\ \Omega_3 &= \omega_3 \alpha_1^{-2} + \omega_4 \alpha_2^{-2} + 2\lambda_2 \alpha_1^- \alpha_2^-, \\ \Omega_4 &= \omega_3 \alpha_1^{+2} + \omega_4 \alpha_2^{+2} + 2\lambda_2 \alpha_1^+ \alpha_2^+, \end{aligned} \tag{4}$$

and the new coupling interaction including the coupling of external field,

$$\begin{aligned} \mu_1 &= \lambda_1(\beta_1^- + \beta_2^-)(\alpha_1^- + \alpha_2^-), \\ \mu_2 &= \lambda_1(\beta_1^+ + \beta_2^+)(\alpha_1^+ + \alpha_2^+), \\ \mu_3 &= \lambda_1(\beta_1^+ + \beta_2^+)(\alpha_1^- + \alpha_2^-), \\ \mu_4 &= \lambda_1(\beta_1^- + \beta_2^-)(\alpha_1^+ + \alpha_2^+). \end{aligned} \tag{5}$$

The Hamiltonian (3) can be rewritten in terms of Heisenberg constants of motion as,

$$\hat{\mathcal{H}} = \omega_f \hat{N} + \Omega_1 \sum_{r=1} \hat{S}_{rr} + \mathcal{H}_{int}. \tag{6}$$

Here, the interaction Hamiltonian  $\mathcal{H}_{int}$  reads,

$$\mathcal{H}_{int} = \delta_1 \hat{S}_{22} + \delta_2 \hat{S}_{33} + \delta_3 \hat{S}_{44} + \hat{a}(\mu_1 \hat{S}_{13} + \mu_2 \hat{S}_{14} + \mu_3 \hat{S}_{23} + \mu_4 \hat{S}_{24}) + h.c., \tag{7}$$

with  $\delta_1 = \sqrt{\Delta_1^2 + 4\lambda_2^2}$ ,  $\delta_2 = \frac{1}{2}(\Delta_3 + \sqrt{\Delta_1^2 + 4\lambda_2^2} - \sqrt{\Delta_2^2 + 4\lambda_2^2})$ ,  $\delta_3 = \frac{1}{2}(\Delta_3 + \sqrt{\Delta_1^2 + 4\lambda_2^2} + \sqrt{\Delta_2^2 + 4\lambda_2^2})$ , and using  $\Delta_3 = 2\omega_f - \omega_1 - \omega_2 + \omega_3 + \omega_4$ . However, the operator  $\hat{N} = \hat{a}^\dagger \hat{a} - \hat{S}_{22} - \hat{S}_{33}$ .

At any time  $t > 0$ , one can assume the wave vector of the interaction Hamiltonian (7) as a follows:

$$|\psi(t)\rangle = \sum_{n=0}^{\infty} (C_1^n(t)|n, l_1\rangle + C_2^n(t)|n, l_2\rangle + C_3^n(t)|n+1, l_3\rangle + C_4^n(t)|n+1, l_4\rangle) \tag{8}$$

The time-dependent Schrödinger equation  $i\frac{\partial}{\partial t}|\psi(t)\rangle = \mathcal{H}_{int}|\psi(t)\rangle$  provides a way to describe the behavior of a quantum system as a function of time, which can be expressed as a system of four ordinary differential equations,

$$\begin{aligned} i\dot{C}_1^n(t) &= v_1 C_1^n(t) + v_2 C_4^n(t), \\ i\dot{C}_2^n(t) &= \delta_1 C_2^n(t) + v_3 C_3^n(t) + v_4 C_4^n(t), \\ i\dot{C}_3^n(t) &= \delta_2 C_3^n(t) + v_1 C_1^n(t) + v_3 C_2^n(t), \\ i\dot{C}_4^n(t) &= \delta_3 C_4^n(t) + v_2 C_1^n(t) + v_4 C_2^n(t), \end{aligned} \tag{9}$$

where  $v_i = \mu_i \sqrt{n+1}$ . It can be assumed that the initial atomic state is prepared in the upper state, while the field is initially in a coherent state  $|\alpha\rangle$  with,

$$|\alpha\rangle = \sum_{n=0}^{\infty} q_n |n\rangle, \quad \text{and} \quad q_n = \frac{\alpha^n}{\sqrt{n!}} e^{-\frac{|\alpha|^2}{2}}. \tag{10}$$

The Laplace transform method provides the exact solution of the time-dependent probability amplitudes in differential eq (9), which can be expressed as,

$$\begin{bmatrix} C_1^n(t) \\ C_2^n(t) \\ C_3^n(t) \\ C_4^n(t) \end{bmatrix} = \begin{bmatrix} a_{11} & a_{12} & a_{13} & a_{14} \\ a_{21} & a_{22} & a_{23} & a_{24} \\ a_{31} & a_{32} & a_{33} & a_{34} \\ a_{41} & a_{42} & a_{43} & a_{44} \end{bmatrix} \begin{bmatrix} e^{\eta_1 t} \\ e^{\eta_2 t} \\ e^{\eta_3 t} \\ e^{\eta_4 t} \end{bmatrix}, \tag{11}$$

with the entries,

$$\begin{bmatrix} a_{1j} \\ a_{2j} \\ a_{3j} \\ a_{4j} \end{bmatrix} = \frac{q_n}{\eta_j \eta_{jk} \eta_{jl}} \begin{bmatrix} h_3 + \eta_j(h_2 + \eta_j(h_1 + \eta_j)) \\ -(k_2 + k_1 \eta_j) \\ l_3 + \eta_j(l_2 + \eta_j l_1) \\ m_3 + \eta_j(m_2 + \eta_j m_1) \end{bmatrix}$$

with  $\eta_{jk} = \eta_j - \eta_k, i \neq j \neq k \neq l = 1, 2, 3, 4$

with

$$\eta_{1,2} = \frac{-x_1}{4} - \frac{z_1}{2} \pm \frac{1}{2} \sqrt{z_2 - \frac{z_3}{4z_1}},$$

$$\eta_{3,4} = \frac{-x_1}{4} + \frac{z_1}{2} \pm \frac{1}{2} \sqrt{z_2 + \frac{z_3}{4z_1}},$$

$$z_1 = \sqrt{f_1 + \frac{f_2}{3f_3} + \frac{f_3}{3}},$$

$$z_2 = 2f_1 - \frac{f_2}{3f_3} - \frac{f_3}{3},$$

$$z_3 = 4x_1 x_2 - x_1^3 - 8x_3,$$

$$f_1 = \frac{x_1^2}{4} - \frac{2x_2}{3},$$

$$f_2 = x_2^2 + 12x_4 - 3x_1 x_3,$$

$$f_3 = \left( \frac{R + \sqrt{R^2 - 4f_2^3}}{2} \right)^{\frac{1}{3}}, \text{ and}$$

$$R = 2x_2^3 + 27(x_3^2 + x_1^2 x_4) - 72x_2 x_4 - 9x_1 x_2 x_3,$$

$$x_1 = i(\delta_1 + \delta_2 + \delta_3),$$

$$x_2 = v_1^2 + v_2^2 + v_3^2 + v_4^2 - \delta_1 \delta_2 - \delta_1 \delta_3 - \delta_2 \delta_3,$$

$$x_3 = i(\delta_1(v_2^2 + v_4^2 - \delta_2 \delta_3) + \delta_2(v_1^2 + v_3^2) + \delta_3(v_1^2 + v_2^2)),$$

$$x_4 = (v_1 v_4 - v_2 v_3)^2 - \delta_1(v_1 \delta_3 + v_2 \delta_2).$$

Also,

$$\begin{aligned}
 h_1 &= i(\delta_1 + \delta_2 + \delta_3), & h_2 &= v_3^2 + v_4^2 - \delta_1(\delta_2 + \delta_3) - \delta_2\delta_3, \\
 h_3 &= i(v_3^2\delta_3 + v_4^2\delta_2 - \delta_1\delta_2\delta_3), \\
 k_1 &= v_1v_3 + v_2v_4, & k_2 &= i(v_2v_4\delta_2 + v_1v_3\delta_3), & l_1 &= -iv_1, \\
 l_2 &= v_1(\delta_1 + \delta_3), \\
 l_3 &= i(v_2v_3v_4 - v_1v_4^2 + v_1\delta_1\delta_3), & m_1 &= -iv_2, \\
 m_2 &= v_2(\delta_1 + \delta_2), & m_3 &= i(v_1v_3v_4 - v_2v_3^2 + v_2\delta_1\delta_2).
 \end{aligned}$$

To study the effect of the driven classical field and detuning parameters on the behavior of coherence, W-function, and phase, it is important to obtain the reduced density operator of the four-level atom sub-state and field sub-state. To do so, one must trace out the field sub-state, yielding the atomic sub-state  $\hat{\rho}_A = \text{Tr}_{\text{field}} |\psi(t)\rangle\langle\psi(t)|$ , where  $|\psi(t)\rangle$  is defined in eq. (8). Thus, the reduced density operator can be found using the transformation (2), which is given by,

$$\hat{\rho}_A = \begin{bmatrix} \rho_{11} & \rho_{12} & \rho_{13} & \rho_{14} \\ \rho_{21} & \rho_{22} & \rho_{23} & \rho_{24} \\ \rho_{31} & \rho_{32} & \rho_{33} & \rho_{34} \\ \rho_{41} & \rho_{42} & \rho_{43} & \rho_{44} \end{bmatrix}, \tag{12}$$

where,

$$\begin{aligned}
 \rho_{11} &= |C_1^n(t)|^2 (\beta_1^-)^2 + 2\beta_1^+ \beta_1^- \text{Re}[C_1^n(t)C_2^{n*}(t)] \\
 &\quad + |C_2^n(t)|^2 (\beta_1^+)^2, \\
 \rho_{22} &= |C_2^n(t)|^2 (\beta_2^-)^2 + 2\text{Re}[C_1^n(t)C_2^{n*}(t)]\beta_2^- \beta_2^+ \\
 &\quad + |C_2^n(t)|^2 (\beta_2^+)^2, \\
 \rho_{33} &= |C_3^n(t)|^2 (\alpha_1^-)^2 + 2\text{Re}[C_3^n(t)C_4^{n*}(t)]\alpha_1^- \alpha_1^+ \\
 &\quad + |C_4^n(t)|^2 (\alpha_1^+)^2, \\
 \rho_{44} &= |C_3^n(t)|^2 (\alpha_2^-)^2 + 2\text{Re}[C_3^n(t)C_4^{n*}(t)]\alpha_2^- \alpha_2^+ \\
 &\quad + |C_4^n(t)|^2 (\alpha_2^+)^2, \\
 \rho_{12} &= \beta_1^- \left( \beta_2^- |C_1^n(t)|^2 + \beta_2^+ C_1^n(t)C_2^{n*}(t) \right) \\
 &\quad + \beta_1^+ \left( \beta_2^- C_2^n(t)C_1^{n*}(t) + \beta_2^+ |C_2^n(t)|^2 \right) = \rho_{21}^*, \\
 \rho_{13} &= \alpha_1^- \left( \beta_1^- C_1^{n+1}(t)C_3^{n*}(t) + \beta_1^+ C_2^{n+1}(t)C_3^{n*}(t) \right) \\
 &\quad + \alpha_1^+ \left( \beta_1^- C_1^{n+1}(t)C_4^{n*}(t) + \beta_1^+ C_2^{n+1}(t)C_4^{n*}(t) \right) + \rho_{31}^*, \\
 \rho_{14} &= \alpha_2^- \left( \beta_1^- C_1^{n+1}(t)C_3^{n*}(t) + \beta_1^+ C_2^{n+1}(t)C_3^{n*}(t) \right) + \alpha_2^+ \\
 &\quad \left( \beta_1^- C_1^{n+1}(t)C_4^{n*}(t) + \beta_1^+ C_2^{n+1}(t)C_4^{n*}(t) \right) = \rho_{41}^*, \\
 \rho_{23} &= \alpha_1^- \left( \beta_2^- C_1^{n+1}(t)C_3^{n*}(t) + \beta_2^+ C_2^{n+1}(t)C_3^{n*}(t) \right) \\
 &\quad + \alpha_1^+ \left( \beta_2^- C_1^{n+1}(t)C_4^{n*}(t) + \beta_2^+ C_2^{n+1}(t)C_4^{n*}(t) \right) = \rho_{32}^*, \\
 \rho_{24} &= \alpha_2^- \left( \beta_2^- C_1^{n+1}(t)C_3^{n*}(t) + \beta_2^+ C_2^{n+1}(t)C_3^{n*}(t) \right) \\
 &\quad + \alpha_2^+ \left( \beta_2^- C_1^{n+1}(t)C_4^{n*}(t) + \beta_2^+ C_2^{n+1}(t)C_4^{n*}(t) \right) = \rho_{42}^*, \\
 \rho_{34} &= \alpha_1^- \left( \alpha_2^- |C_3^n(t)|^2 + \alpha_2^+ C_2^n(t)C_4^{n*}(t) \right) \\
 &\quad + \alpha_1^+ \left( \alpha_2^- C_4^{n+1}(t)C_3^{n*}(t) + \alpha_2^+ |C_4^n(t)|^2 \right) = \rho_{43}^*,
 \end{aligned} \tag{13}$$

Likewise, the reduced density field sub-state system can be obtained by tracing out the atomic sub-state, which is given by,

$$\begin{aligned}
 \hat{\rho}_{\text{field}} &= \sum_{n,m=0}^{\infty} \left( (C_1^n(t)C_1^{m*}(t) + C_2^n(t)C_2^{m*}(t))|n\rangle\langle m| \right. \\
 &\quad \left. + (C_3^n(t)C_3^{m*}(t) + C_4^n(t)C_4^{m*}(t))|n+1\rangle\langle m+1| \right) \tag{14}
 \end{aligned}$$

Hereinafter, we shall employ the final reduced density atomic and field states to discuss coherence, non-classicality, and phase jumps.

### 3 Relative entropy of coherence

Relative entropy of coherence (REC) is a measure of the amount of quantum coherence present in a quantum state, and it is defined as the relative entropy between the given state  $\hat{\rho}$  and the closest incoherent state, say all diagonal entries of a quantum state  $\hat{\rho}$  [14]. This measure has been widely applied in various areas of quantum information, such as entanglement theory, quantum cryptography, and quantum computing. In particular, REC has been used to quantify the amount of entanglement present in a bipartite system [32], to study the security of quantum key distribution protocols [33], and to characterize the performance of teleportation protocol [34]. Moreover, REC has been useful for understanding the dynamics of decoherence in open systems [35], allowing us to acquire a better insight into the effects of decoherence on the quantum nature of a system. These make REC a powerful tool for probing and understanding the behavior of quantum systems. REC is defined via von Neumann entropy as [14],

$$C_{Re} = S_d - S, \tag{15}$$

where  $S_d = -\text{Tr} \hat{\rho}_d \log \hat{\rho}_d$  with  $\hat{\rho}_d$  is the diagonal entries of a quantum state  $\hat{\rho}$ , and  $S = -\text{Tr} \hat{\rho} \log \hat{\rho}$ .

In figure 1, we used the atomic density state in Eq. (12) to investigate the impact of various detuning parameters and external classical field values on the coherence of a system, as measured by the temporal of REC with  $\alpha = 5$ . Our results demonstrate a direct correlation between these parameters and the degree of coherence, with some parameter values leading to maximum coherence and others to minimum coherence. This suggests that these parameters can be manipulated to control the coherence of the system, allowing users to maximize or minimize the degree of coherence as needed. This can be of great use in the development of quantum information processing, where a high degree of coherence is usually preferred. In general, the level of coherence of a system at the onset of an interaction is impacted by the intensity of the external classical field.

It is shown that the REC is zero for certain values of  $\lambda_2$ , as seen in figures 1 (a, b), and grows as  $\lambda_2$  increases (figures 1 (c, d)). As seen in figure 1. (a), the coherence of an atom–field interaction decreases with increasing the interaction time when the atom–field interaction is affected by small values of classical field and detuning parameters. This can be attributed to the energy exchange between the atom and the field, which causes the system to become less coherent. However, when the detuning parameters increase and the external field strength decreases, as seen in figure 1. (b), the maximum bounds of coherence increase and the minimum bounds decrease. This suggests that the increase in detuning parameters results in an increase in dispersion, which in turn leads to an expansion in the amplitude of the  $C_{Re}$ . This phenomenon can be explained by the fact that the atom–field interaction becomes increasingly more non-resonant, and therefore the energy exchange between them is reduced, leading to an overall increase in the coherence of the system. When considering the effect of a large classical field value (figure 1. (c)), it is apparent that the maximum bounds of relative coherence decrease as the interaction time increases, and the number of oscillations decreases with a small amplitude. The external classical field reinforces the system at specific values and reduces fluctuations in relative

coherence. For example, at  $\lambda_2 = 30$  and different values of detunings, the relative coherence is a straight line at  $\ln 2$ . Furthermore, figure 1. (d) indicates that higher values of the classical field and detunings can increase the coherence of the system, resulting in an extended amplitude of the coherence. This phenomenon is further supported by the fact that larger values of the classical field are capable of counteracting the destabilizing effects of the detuning parameters, thus contributing to the overall stability of the system.

#### 4 The Wigner function (W-function)

The temporal evolution of the Wigner function (W-function) is a key characteristic of the atom–field interaction and can be used to measure the non-classicality of the system [36]. The W-function is a quasiprobability distribution in phase space that describes the quantum state of a system, and its evolution over time is determined by the Moyal equation [37]. By looking at the shape of the W-function and its evolution over time, one can measure the amount of quantum correlation present in the system. For example, the

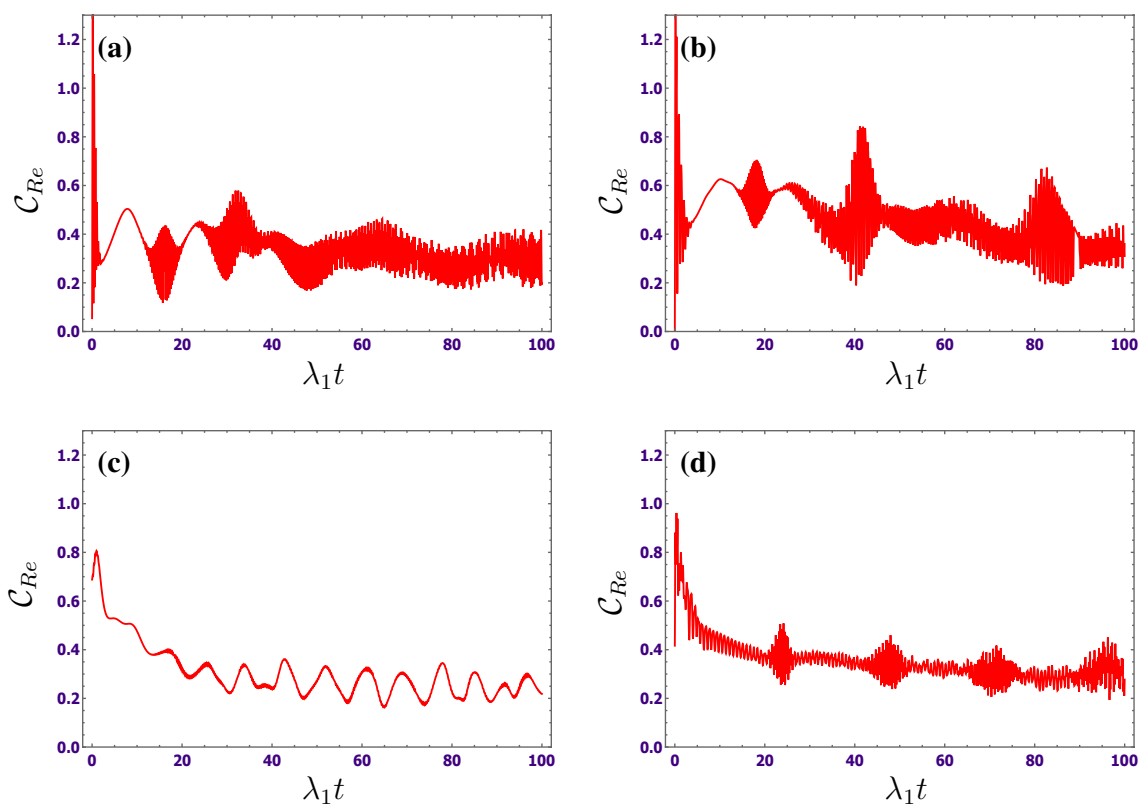


**Fig. 1** The dynamical behavior of REC  $C_{Re}$  as a function of  $\lambda_1 t$  with  $\alpha = 5$ . (a)  $\Delta_1 = 1, \Delta_2 = 0.1, \Delta_3 = 0.1, \lambda_2 = 0.1$  (b)  $\Delta_1 = 10, \Delta_2 = 2, \Delta_3 = 5, \lambda_2 = 0.1$  (c)  $\Delta_1 = 1, \Delta_2 = 0.1, \Delta_3 = 0.1, \lambda_2 = 5$  and (d)  $\Delta_1 = 10, \Delta_2 = 2, \Delta_3 = 5, \lambda_2 = 5$



W-function can take on negative values, which is a signature of entanglement [38]. For the reduced field density state, one can defined W-function ( $\mathcal{W}(\beta)$ ) as [39, 40],

$$\mathcal{W}(\beta) = \frac{2}{\pi} \sum_{k=1}^{\infty} (-1)^k \langle k | D^\dagger(\beta) \hat{\rho}_{\text{field}} D(\beta) | k \rangle, \tag{16}$$

where  $D(\beta)$  is a displaced number state with  $\beta = x + iy$ , and  $\rho_{\text{field}}$  is the reduced density matrix of the field in eq.(14). For our system, one may obtain the W-function as [41],

$$\mathcal{W}(\beta) = \frac{2}{\pi} e^{-|\beta|^2} \sum_{k=1}^{\infty} \sum_{n=1}^{\infty} (-1)^k \left( |C_1^n + C_2^n D_{k,n}(-\beta)|^2 + |C_3^n + C_4^n D_{k,n+1}(-\beta)|^2 \right), \tag{17}$$

here,

$$D_{k,n}(\beta) = \sqrt{\frac{n!}{k!}} (\beta^*)^{k-n} L_n^{k-n}(|\beta|^2), \tag{18}$$

The W-function has been demonstrated to be a reliable two-fold measure for assessing the quantum and classical properties of a system. Negative values of the W-function are indicative of quantumness, while positive values are suggestive of classicality or minimal uncertainty. In figure 2, we present

the effects of varying detuning parameters and different intensities of the coupling of the classical field  $\lambda_2$  on the Wigner function for a system with a scaled interaction time of  $\lambda_1 t = 5$ , which is in the middle of the collapse period in atomic inversion [42]. This analysis serves to illustrate the utility of the W-function as an effective tool for analyzing both the quantum and classical characteristics of a system. Under the same conditions as those used in figure 1, figure 2 (a) shows the W-function for the field subsystem with a small value of the detuning parameter and the coupling of the classical field. This resulted in a quantum behavior that was confined to the middle of the phase space, while the classicality of the system was visible in the middle of the phase space and around points  $(2, \pm 4)$ . This indicates that quantum behavior is confined to the middle of the phase space, while classicality is visible in both the middle and around points  $(2, \pm 4)$ . The results of figure 2 (b) display that an increase in the detuning parameters can lead to a substantial change in the W-function, where one of the separated peaks increases, while the other disappears and negative values decrease [43]. This suggests that classicality increases with large detuning, being limited to positive values of  $\beta$ , i.e.,  $Im[\beta]$  and  $Re[\beta] > 0$ . This finding is consistent with previous research which has established that large detuning can increase classical correlations. It is noteworthy that these correlations are only observed for positive values of  $\beta$ , thus highlighting the importance

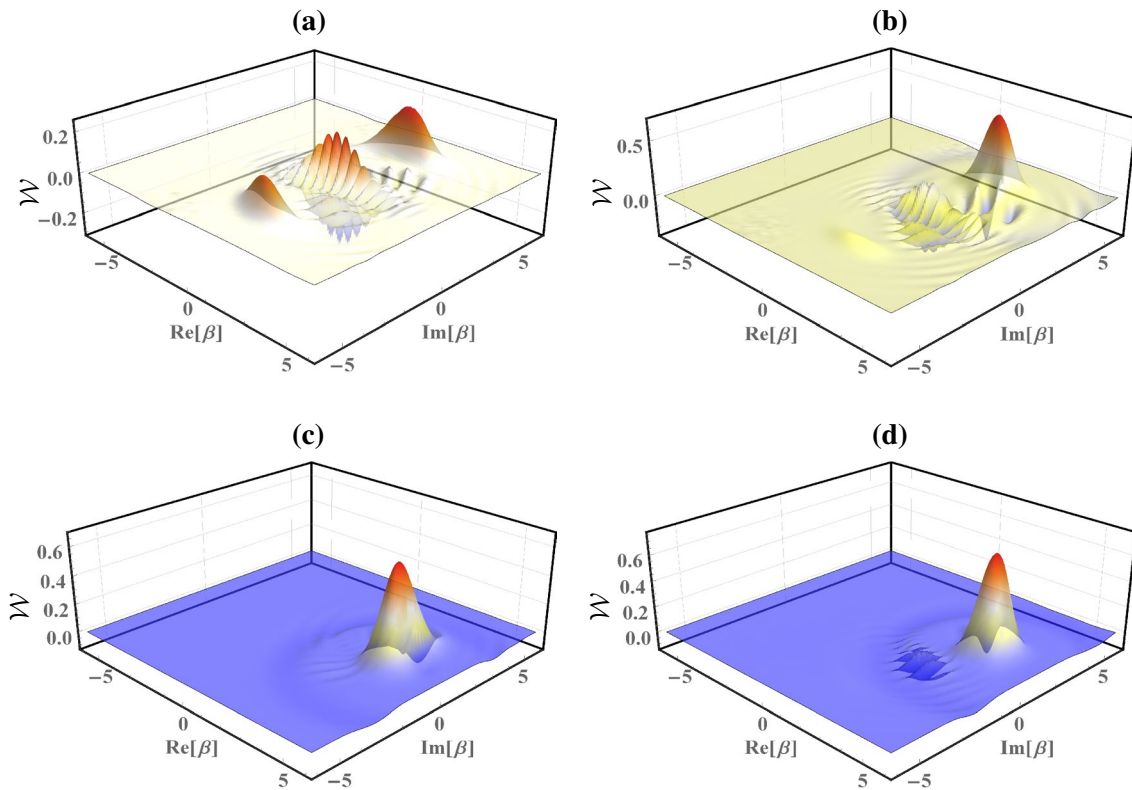


**Fig. 2** The 3D plot of W-function  $\mathcal{W}$  as a function of  $\beta$  where  $\lambda_1 t = 5$  and  $\alpha = 4$ . The detuning parameters and the coupling of classical field are the same as figure 1

of selecting appropriate parameters to achieve the desired behavior. As figures 2 (c and d) illustrate, an increase in the classical field leads to a subsequent rise in classical correlation and a decrease in quantum correlation. Furthermore, a single positive peak appears at (4,2) for large detuning and (4,0) for smaller detuning, while the diffusion peaks in the middle of phase space have dissipated. This implies that the classicality of the system increases with increasing detuning, while the coupling of the classical field suppresses the negative behavior in the middle of the phase space. Consequently, large detuning can result in an enhancement of classical correlations and the emergence of distinct positive peaks in the middle of phase space.

## 5 Pancharatnam phase

The Pancharatnam phase is a mathematical concept introduced by S. Pancharatnam in 1956 [44], which can be used to quantify the relative phase between two waveforms. This concept has the potential to be employed in order to measure the phase space of a system and is related to the polarization of light. This has been found to be particularly useful for the analysis of complex systems, as well as for applications such as quantum computing, where it can be used to quantify the quantum phase of a qubit and quantum

electrodynamics systems [45–49]. Furthermore, its potential applications extend to the study of optical properties of materials, such as the polarization of light [50]. The Pancharatnam phase encompasses the dynamical phase and the geometric phase, which is calculated as the phase acquired during the change in the wave function from the initial wave vector  $|\psi(0)\rangle$  to the final wave vector  $|\psi(t)\rangle$ , which is expressed as [51],

$$\Phi(t) = \arg (\langle \psi(0) | \psi(t) \rangle), \quad (19)$$

The effects of classical field parameters and the detuning parameters on the Pancharatnam phase are clearly visible in figure 3. As shown in figures 3(a) and (c), the classical field parameter has a significant impact on the oscillation of the phase, causing a periodic saw-tooth type of oscillation in cases where the value of  $\lambda_2$  is lower, and a reduced number of oscillations when the effect of the classical field is larger. This indicates the phase's capability of changing rapidly, leading to brief periods of artificial phase jumps in the lower values of the external classical field. In contrast, the effect of the detuning parameters amplifies the swift fluctuation over brief periods, thus raising the detuning effect produces random phase jumps. However, by augmenting the external classical field, the leap of the function  $\Phi(t)$  diminishes with time. This confirms that the external classical field stabilizes

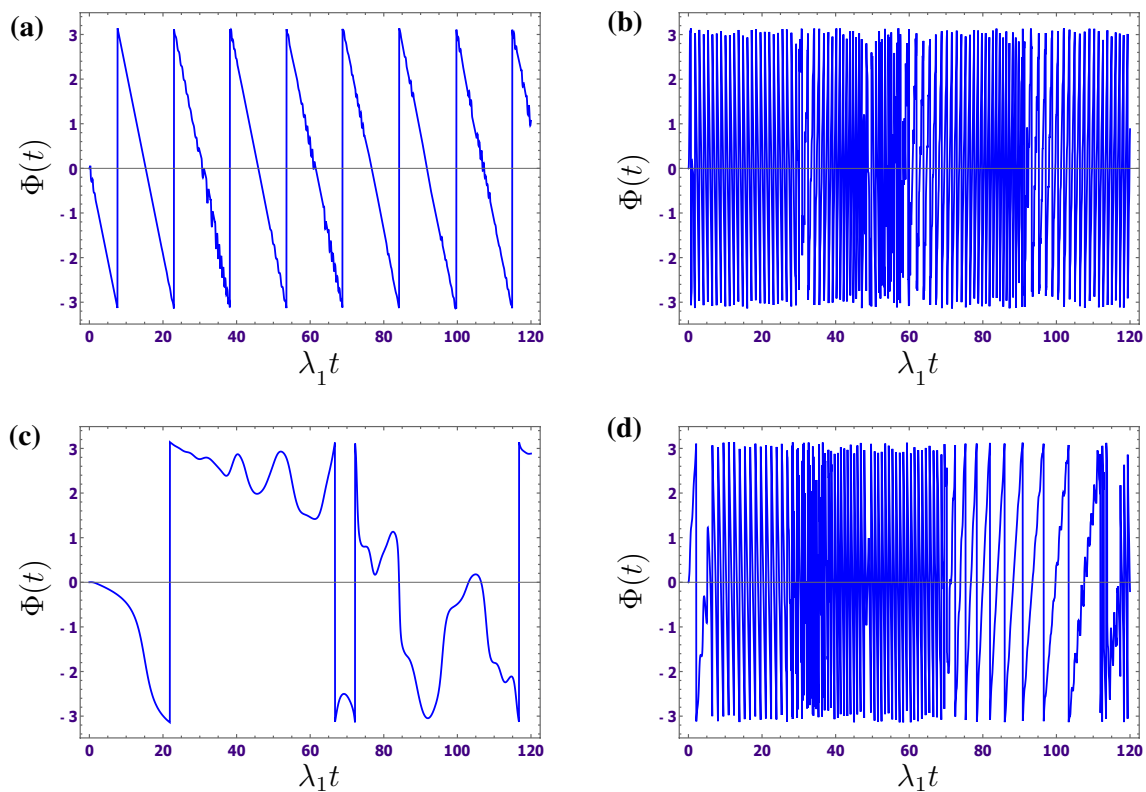


**Fig. 3** The dynamical behavior of Pancharatnam phase  $\Phi(t)$  as a function of  $\lambda_1 t$  with the same parameters as displayed in figure 1

the interaction between the field and matter after a period of interaction.

## 6 Conclusions

This paper presented a study of a single four-level atom in a W-configuration interacting locally with a single-mode quantized cavity field. The initial cavity field is assumed to be in a coherent state, and the atomic system is taken to be in the upper state. By employing exact solutions of the Schrödinger equation under certain canonical conditions of dressed states, we are able to obtain the exact solution without making any assumptions. Subsequently, we investigate the effects of detuning parameters and an external classical field on coherence, non-classicality, and phase space. Our findings suggest that these three phenomena can be modified by the strength of the classical field and the detuning parameters, thereby allowing for controlled manipulation of relative coherence, Wigner function, and Pancharatnam phase.

The effect of detuning on the behaviors of coherence, quantumness, and Pancharatnam phase is discussed. It is demonstrated that the rate of decrease/increase of these three phenomena is contingent upon the detuning parameter. As the detuning increases, the lower bounds of coherence and negative values of Wigner function are observed to diminish. On the other hand, Pancharatnam phase exhibits a rapid oscillation as detuning increases, suggesting that it is more sensitive to changes in detuning than coherence and quantumness.

The effects of varying values of the external field on the general behaviors of coherence, non-classicality, and phase space in the presence of detuning parameters are investigated. We find that as the strength of the classical field increases, the effect of the detuning parameters is reduced, allowing the quantum system to remain stable at large values of the classical field. Additionally, our results indicate that the maximum bounds of coherence decrease, the classicality of the system increases, and the phase jumps decrease as the external field increases.

**Funding** Openaccess funding provided by The Science, Technology & Innovation Funding Authority (STDF) in cooperation with The Egyptian Knowledge Bank (EKB).

**Open Access** This article is licensed under a Creative Commons Attribution 4.0 International License, which permits use, sharing, adaptation, distribution and reproduction in any medium or format, as long as you give appropriate credit to the original author(s) and the source, provide a link to the Creative Commons licence, and indicate if changes were made. The images or other third party material in this article are included in the article's Creative Commons licence, unless indicated otherwise in a credit line to the material. If material is not included in the article's Creative Commons licence and your intended use is not permitted by statutory regulation or exceeds the permitted use, you will

need to obtain permission directly from the copyright holder. To view a copy of this licence, visit <http://creativecommons.org/licenses/by/4.0/>.

## References

1. W. P. Schleich (2011) Quantum optics in phase space. John Wiley & Sons,
2. I.I. Rabi, Space quantization in a gyrating magnetic field. *Phys. Rev.* **51**, 652–654 (1937)
3. Y. Yan, T.T. Ergogo, Z. Lu, L. Chen, J. Luo, Y. Zhao, Lamb shift and the vacuum Rabi splitting in a strongly dissipative environment. *J. Phys. Chem. Lett.* **12**(40), 9919–9925 (2021)
4. E.T. Jaynes, F.W. Cummings, Comparison of quantum and semiclassical radiation theories with application to the beam maser. *Proc. IEEE* **51**(1), 89–109 (1963)
5. F. Deppe, M. Mariani, E. Menzel, A. Marx, S. Saito, K. Kakuyanagi, H. Tanaka, T. Meno, K. Semba, H. Takayanagi et al., Two-photon probe of the Jaynes-Cummings model and controlled symmetry breaking in circuit QED. *Nat. Phys.* **4**(9), 686–691 (2008)
6. A.M. Abdel-Hafez, A.M.M. Abu-Sitta, A.-S.F. Obada, A generalized Jaynes-Cummings model for the N-level atom and (N- 1) modes. *Phys. A* **156**(2), 689–712 (1989)
7. A.-S.F. Obada, E.M. Khalil, S. Abdel-Khalek, S.I. Ali, New features of a single-mode nonlinear Stark shift in the presence of phase damping. *Opt. Commun.* **285**(10–11), 2675–2681 (2012)
8. M.S. Abdalla, A.-S.F. Obada, E.M. Khalil, S.I. Ali, The influence of phase damping on a two-level atom in the presence of the classical laser field. *Laser Phys.* **23**(11), 115201 (2013)
9. A.-B.A. Mohamed, Non-local correlations via Wigner-Yanase skew information in two SC-qubit having mutual interaction under phase decoherence. *Europ. Phys. J. D* **71**, 1–8 (2017)
10. M.F. Alotaibi, E.M. Khalil, S. Abdel-Khalek, M.Y. Abd-Rabbou, M. Omri, Effects of the vibrating graphene membrane and the driven classical field on an atomic system coupled to a cavity field. *Results Phys.* **31**, 105012 (2021)
11. M.F. Alotiabi, E.M. Khalil, M.Y. Abd-Rabbou, Dynamics of an atomic system associated with a cavity-optomechanical system. *Results Phys.* **37**, 105540 (2022)
12. H.S. Alqannas, S. Abdel-Khalek, Physical and nonclassical properties of the interaction between a four-level atom and field in coherent state of Morse potential. *Opt. Quant. Electron.* **51**, 1–10 (2019)
13. E.M. Khalil, H. Abu-Zinadah, M.Y. Abd-Rabbou, Influence of an external classical field on a four-level atom inside a quantized field. *Symmetry* **14**(4), 811 (2022)
14. T. Baumgratz, M. Cramer, M.B. Plenio, Quantifying coherence. *Phys. Rev. Lett.* **113**, 140401 (2014)
15. Y.-T. Wang, J.-S. Tang, Z.-Y. Wei, S. Yu, Z.-J. Ke, X.-Y. Xu, C.-F. Li, G.-C. Guo, Directly measuring the degree of quantum coherence using interference fringes. *Phys. Rev. Lett.* **118**, 020403 (2017)
16. M.Y. Abd-Rabbou, S.I. Ali, M.M.A. Ahmed, Enhancing the information of nonlinear SU (1, 1) quantum systems interacting with a two-level atom. *Opt. Quant. Electron.* **54**(9), 548 (2022)
17. S.I. Ali, Influence of deformed cavity field and atomic dipole interaction on the quantum correlations of two-qubit system. *Opt. Quant. Electron.* **55**(1), 47 (2023)
18. N.I. Mohammed, H.M. Abdelsalam, S. Almalki, M.Y. Abd-Rabbou, S. Abdel-Khalek, E.M. Khalil, Witnessing quantum correlations in two coupled quantum dots under intrinsic decoherence. *Alexand. Eng. J.* **69**, 521–527 (2023)
19. M. Abd-Rabbou, N. Metwally, M. Ahmed, A.-S.F. Obada, Decoherence and quantum steering of accelerated qubit-qutrit system. *Quant. Info. Process.* **21**(10), 363 (2022)



20. M.Y. Abd-Rabbou, S.I. Ali, N. Metwally, Detraction of decoherence that arises from the acceleration process. *JOSA B* **40**(3), 585–593 (2023)
21. E. Wigner, On the quantum correction for thermodynamic equilibrium. *Phys. Rev.* **40**, 749–759 (1932)
22. G. Gradoni, S.C. Creagh, G. Tanner, C. Smartt, D.W. Thomas, A phase-space approach for propagating field-field correlation functions. *New J. Phys.* **17**(9), 093027 (2015)
23. N. Metwally, M. Abd-Rabbou, A.-S. F. Obada, M. M. A. Ahmed (2019) Wigner function of accelerated and non-accelerated Greenberger–Horne–Zeilinger state, In 2019 8th International Conference on Modeling Simulation and Applied Optimization (ICMSAO), pp. 1–5, IEEE,
24. M.Y. Abd-Rabbou, N. Metwally, M. Ahmed, A.-S.F. Obada, Wigner distribution of accelerated tripartite W-state. *Optik* **208**, 163921 (2020)
25. M. Walschaers, C. Fabre, V. Parigi, N. Treps, Entanglement and Wigner function negativity of multimode non-Gaussian states. *Phys. Rev. Lett.* **119**, 183601 (2017)
26. T.K. Mavrogordatos, Visualizing the breakdown of quantum multimodality in coherently driven light-matter interaction. *Phys. Rev. A* **106**, 013711 (2022)
27. M.F. Alotaibi, E.M. Khalil, M.Y. Abd-Rabbou, M. Marin, The classicality and quantumness of the driven qubit-photon-magnon system. *Mathematics* **10**(23), 4458 (2022)
28. M.Y. Abd-Rabbou, N. Metwally, M. Ahmed, A.-S.F. Obada, Wigner function of noisy accelerated two-qubit system. *Quant. Inf. Process.* **18**, 1–19 (2019)
29. P.-G. Zhong, C. Li, Y. Wang, J. Song, S.-T. Liu, Y.-Y. Jiang, Y. Xia, Quantum phase transitions triggered by a four-level atomic system in dissipative environments. *Phys. Rev. A* **99**, 043829 (2019)
30. F. Wen, H. Zheng, X. Xue, H. Chen, J. Song, Y. Zhang, Electromagnetically induced transparency-assisted four-wave mixing process in the diamond-type four-level atomic system. *Opt. Mater.* **37**, 724–726 (2014)
31. S. Li, X. Yang, X. Cao, C. Zhang, C. Xie, H. Wang, Enhanced cross-phase modulation based on a double electromagnetically induced transparency in a four-level tripod atomic system. *Phys. Rev. Lett.* **101**, 073602 (2008)
32. A. Streltsov, U. Singh, H.S. Dhar, M.N. Bera, G. Adesso, Measuring quantum coherence with entanglement. *Phys. Rev. Lett.* **115**, 020403 (2015)
33. J. Ma, Y. Zhou, X. Yuan, X. Ma, Operational interpretation of coherence in quantum key distribution. *Phys. Rev. A* **99**, 062325 (2019)
34. M. Omri, M.Y. Abd-Rabbou, E.M. Khalil, S. Abdel-Khalek, Thermal information and teleportation in two-qutrit Heisenberg XX chain model. *Alex. Engin. J.* **61**(10), 8335–8342 (2022)
35. Z. He, H.-S. Zeng, Y. Li, Q. Wang, C. Yao, Non-markovianity measure based on the relative entropy of coherence in an extended space. *Phys. Rev. A* **96**, 022106 (2017)
36. A. Kenfack, K. Życzkowski, Negativity of the Wigner function as an indicator of non-classicality. *J. Opt. B* **6**(10), 396 (2004)
37. J. E. Moyal (1949) Quantum mechanics as a statistical theory. In: *Math. Proc. Camb. Phil. Soc.*, Cambridge University Press, pp. 99–124,
38. R. McConnell, H. Zhang, J. Hu, S. Čuk, V. Vuletić, Entanglement with negative Wigner function of almost 3,000 atoms heralded by one photon. *Nature* **519**(7544), 439–442 (2015)
39. C. Gerry, P.L. Knight, *Introductory quantum optics* (Cambridge University Press, Oxford, 2005)
40. H.A. Hessian, A.B.A. Mohamed, Quasi-probability distribution functions for a single trapped ion interacting with a mixed laser field. *Laser phys.* **18**, 1217–1223 (2008)
41. A.-B.A. Mohamed, H. Eleuch, Quasi-probability information in a coupled two-qubit system interacting non-linearly with a coherent cavity under intrinsic decoherence. *Sci. Rep.* **10**(1), 13240 (2020)
42. A.B. Mohamed, H. Eleuch, Non-classical effects in cavity qed containing a nonlinear optical medium and a quantum well: Entanglement and non-gaussianity. *Europ. Phys. J. D* **69**, 1–8 (2015)
43. M.Y. Abd-Rabbou, E.M. Khalil, M.M.A. Ahmed, A.S.F. Obada, External classical field and damping effects on a moving two level atom in a cavity field interaction with kerr-like medium. *Int. J. Theor. Phys.* **58**, 4012–4024 (2019)
44. S. Pancharatnam (1956) Generalized theory of interference, and its applications: Part I. coherent pencils,” in *Proceedings of the Indian Academy of Sciences-Section A*, vol. 44, pp. 247–262, Springer India New Delhi,
45. V. Vedral, Geometric phases and topological quantum computation. *Int. J. Quant. Inf.* **1**(01), 1–23 (2003)
46. X.-Y. Xu, Q.-Q. Wang, M. Heyl, J.C. Budich, W.-W. Pan, Z. Chen, M. Jan, K. Sun, J.-S. Xu, Y.-J. Han et al., Measuring a dynamical topological order parameter in quantum walks. *Light* **9**(1), 7 (2020)
47. A.B.A. Mohamed, A.S.F. Obada, Asymptotic geometric phase and purity for phase qubit dispersively coupled to lossy lc circuit. *Ann. Phys.* **326**(9), 2369–2376 (2011)
48. A.B.A. Mohamed, H. Eleuch, Geometric phase in cavity QED containing a nonlinear optical medium and a quantum well. *J. Mod. Opt.* **62**(19), 1630–1637 (2015)
49. A.-B.A. Mohamed, A. Farouk, A.-H.A. Aty, H. Eleuch, Robustness of generated geometric phase of quantum wells in two open waveguide-coupled optical cavities. *IEEE Acc.* **8**, 158745–158751 (2020)
50. W. Dultz, D. T. Darmstadt (1995) Pancharatnam’s phase in polarization optics. In *Advanced Electromagnetism: Foundations, Theory and Applications*, pp. 357–375, World Scientific Singapore,
51. Q. Lawande, S. Lawande, A. Joshi, Pancharatnam phase for a system of a two-level atom interacting with a quantized field in a cavity. *Phys. Lett. A* **251**(3), 164–168 (1999)